Phase Separation in Binary Mixtures of Bipolar and Monopolar Lipid Dispersions Revealed by ²H NMR Spectroscopy, Small Angle X-Ray Scattering, and Molecular Theory

David P. Brownholland,[†] Gabriel S. Longo,[‖] Andrey V. Struts,[‡] Matthew J. Justice,[¶] Igal Szleifer,[††] Horia I. Petrache,[¶] Michael F. Brown,[‡§] and David H. Thompson[†*]

[†]Department of Chemistry, Purdue University, West Lafayette, Indiana; [‡]Department of Chemistry and [§]Department of Physics, University of Arizona, Tucson, Arizona; [¶]Department of Physics, Indiana University-Purdue University Indianapolis, Indianapolis, Indiana; [‖]International School for Advanced Studies and the Abdus Salam International Centre for Theoretical Physics, Trieste, Italy; and [††]Department of Biomedical Engineering, Northwestern University, Evanston, Illinois

ABSTRACT   Binary mixtures of $C_{20}BAS$ and POPC membranes were studied by solid-state ²H NMR spectroscopy and small angle x-ray scattering (SAXS) over a wide range of concentrations and at different temperatures. Three specifically deuterated $C_{20}BAS$ derivatives—[1′,1′,20′,20′-²H₄]$C_{20}BAS$, [2′,2′,19′,19′-²H₄]$C_{20}BAS$, and [10′,11′-²H₂]$C_{20}BAS$—combined with protiated 1-palmitoyl-2-oleoyl-*sn*-glycero-3-phosphocholine (POPC), as well as membranes containing POPC-d₃₁ and fully protiated bolalipid, were used in NMR experiments to obtain structural information for the mixtures. The ²H NMR spectra of [10′,11′-²H₂]$C_{20}BAS$/POPC membrane dispersions reveal that the bolalipid is predominantly in the transmembrane conformation at high bolalipid concentrations (100, 90, and 70 mol %). At ≤50 mol % $C_{20}BAS$, smaller quadrupolar couplings appear in the spectra, indicating the presence of U-shaped conformers. The proportion of U-shaped bolalipids increases as the amount of POPC in the membrane increases; however, the transmembrane component remains the dominant bolalipid conformation in the membrane even at 45°C and 10 mol % $C_{20}BAS$, where it accounts for ~50% of the bolalipid population. The large fraction of $C_{20}BAS$ transmembrane conformers, regardless of the $C_{20}BAS$/POPC ratio, together with the findings from molecular mean-field theory calculations, suggests the coexistence of phase-separated bolalipid-rich domains and POPC-rich domains. A single lamellar repeat distance was observed in SAXS experiments corresponding to the average repeat spacing expected for $C_{20}BAS$- and POPC-rich domains. These observations are consistent with the presence of microphase-separated domains in the mixed membrane samples that arise from POPC-$C_{20}BAS$ hydrophobic mismatch.

INTRODUCTION

A growing body of evidence suggests that cell membranes are complex, heterogeneous liquid-crystalline materials with phase-separated lipid domains. Because of the difficulties involved in studying these phenomena in their native membrane context, most investigators have relied on various model membrane systems to help elucidate the physical properties, dynamics, composition, and significance of these structures (1–8). Two types of lipid domains have been detected using model membranes. The first is produced by a simple binary mixture of lipids with significantly different melting transition temperatures (T_m). At temperatures between the two melting transitions, the lipid with the lower T_m adopts a liquid-crystalline (L_α) or liquid-disordered (l_d) phase that tends to separate from the lipid with the higher T_m, which adopts a more ordered and relatively immobile gel phase (L_β). L_β/l_d phase immiscibility is not believed to be relevant to the functional state of biological membranes. Model membranes composed of ternary mixtures of two lipids with different melting transitions enriched with cholesterol (typically unsaturated lipids mixed with either saturated lipids or sphingomyelin) can also produce two phase-separated domains: an l_d phase and a liquid-ordered (l_o) phase, the latter of which is considered analogous to so-called lipid rafts in cell membranes. The l_o phase is a hybrid of the L_β and L_α phases, i.e., it contains lipids with a high-degree of order, as formed in the L_β phase, while maintaining the lateral fluidity characteristic of the L_α phase (3,8). A variety of techniques have been used to detect lipid domains in model membranes (8–14); however, many fundamental questions about lipid domains in cell membranes remain concerning their mechanism of formation, their size and lifetime, and the factors that may influence their ability to include or exclude membrane proteins (3,5,15).

Phase separation in membranes is also relevant for lipid membrane-based technologies. To realize the promise of these technologies, researchers are developing new lipids and polymers to create rugged membrane constructs that maintain membrane protein function. Understanding how these new materials interact with lipid membranes is critical for developing stable and functional membrane-based devices. Bipolar lipids, or bolalipids, constitute a novel class of phospholipids that are currently under investigation for these purposes (16–21). Bolalipids are naturally found in the membranes of *Archaea* (22,23) and enable these organisms to survive under harsh conditions, such as extreme temperatures, high salt concentration, low pH, and anaerobic

conditions due to the unique isoprenoid chains that are ether-linked to the glyceryl- and glycal-based polar headgroups (22,24) present on the inner and outer surfaces, respectively, of their plasma membrane. These hydrolysis-resistant membrane-spanning alkyl chains are believed to be responsible for the enhanced physical and chemical stability of *Archaea*, and also provide resistance to bilayer membrane delamination within the extreme environment in which they thrive. The enhanced stability of bolalipid membranes has been employed in the development of planar supported membranes (17,25,26), gene and vaccine delivery vehicles (27–30), functional reconstitution of integral membrane proteins (IMPs) (18,19,31,32), and as molecular fossils (33). Major impediments to the more widespread use of bolalipids in membrane-based biosensors are the cost and difficulties involved in either purifying or totally synthesizing discrete *Archaeal* lipid species. These challenges have prompted researchers to focus on the development of archaeal lipid mimics, which contain many of the desired properties of natural bolalipids (23,25,30,34–38).

Kim et al. (18) and Febo-Ayala et al. (19) synthesized a small library of synthetic bolalipids designed to generate stable planar supported membranes with reconstituted IMPs for biosensors. Previous work established that bolalipid membranes are physically robust, chemically stable, less permeable than membranes composed of monopolar lipids, and retain lateral mobilities that are similar to the conventional monopolar lipids—an essential feature of membrane dynamics that is likely to be necessary for the functional reconstitution of IMPs (18,20,26,39). The average segmental order parameters at the $C_{(1:20)}$, $C_{(2:19)}$, and $C_{(10:11)}$ positions of deuterated $C_{20}BAS$ (Fig. 1 A) were also obtained in previous experiments (21). Those experiments showed that $C_{20}BAS$ bolalipid membranes, unlike typical bilayer membranes, are highly ordered, especially at the $C_{10,11}$ positions, in the center of the membrane (21). It should also be noted that most synthetic and naturally occurring bolalipids have sufficient flexibility to exist in two conformational states in the membrane: a transmembrane conformation with two polar headgroups on opposite leaflets of the membrane, and a U-shaped conformation with both headgroups residing on the same leaflet. However, several experimental and theoretical studies have suggested that bolalipids predominantly adopt a transmembrane conformation in the membrane (16,21,40–42).

Functional reconstitution experiments with the IMP Ste14p in membranes mixed with bolalipids and monopolar lipids indicated that bolalipids may form heterogeneous membranes with monopolar lipids in a composition-dependent manner (19). Longo and co-workers (42) recently used molecular mean-field theory to evaluate mixtures of C_{20}-based bolalipids and monopolar lipids of varying lengths. They showed that phase separation between bolalipids and monopolar lipids occurs when the membrane thicknesses of two lipids differ significantly (42). We inferred from those findings that two distinct lipid domains (Fig. 1 B) should form after $C_{20}BAS$
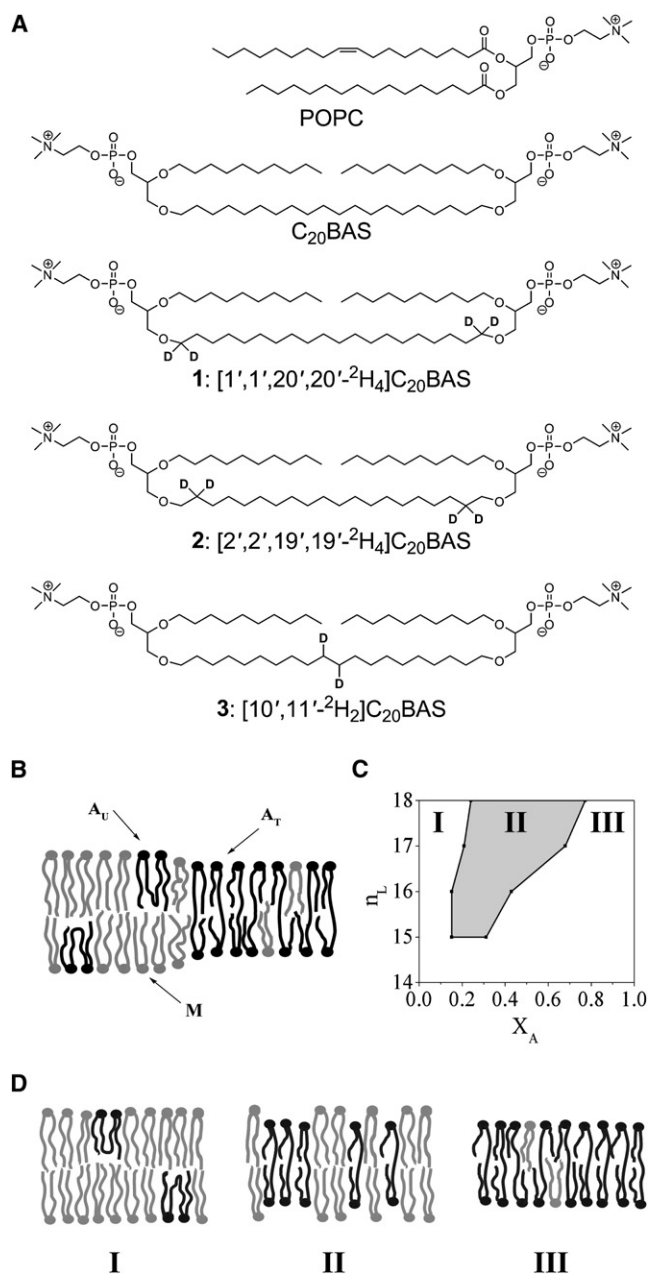

FIGURE 1 (A) Structures of POPC, $C_{20}BAS$, and deuterated $C_{20}BAS$ derivatives 1–3. (B) Schematic representation of the predicted phase separation for a mixed $C_{20}BAS$/POPC lipid membrane. The bolalipid-rich domain consists of transmembrane bolalipids (A_T) and a small molar ratio of POPC (M). The monopolar lipid-rich domain consists of POPC with a small molar ratio of U-shaped bolalipids (A_U). (C) Predicted miscibility diagram showing the regime of lipid mixtures where phase separation between fluid phase $C_{20}BAS$ and monopolar lipids (adapted from (42)) is expected (gray shaded area). X_A is the molar fraction of $C_{20}BAS$, and n_L is the number of carbons in the hydrophobic chain of the monopolar lipid. (D) Diagram of various membrane lipid configurations in different regions of the miscibility diagram. I = POPC-rich phase with U-shaped $C_{20}BAS$ conformations; II = mixture of $C_{20}BAS$ and POPC that generates significant hydrophobic mismatch leading to a separation into type I and III domains; III = $C_{20}BAS$-rich phase with modest POPC content (predominantly transmembrane $C_{20}BAS$ with some U-conformers, especially at higher temperatures).

bolalipid is mixed with 1-palmitoyl-2-oleoyl-*sn*-glycero-3-phosphocholine (POPC; Fig. 1 *A*) at intermediate bipolar/monopolar lipid ratios (Fig. 1 *C*). A 3-nm-thick domain containing predominantly transmembrane $C_{20}BAS$ and a small percentage of POPC should coexist with a second type of domain (4-nm thick) containing predominantly POPC and a low molar ratio of $C_{20}BAS$ in a U-shaped conformer (Fig. 1, *B* and *D*). Order parameters for the C-^{2}H bonds in the transmembrane region of $C_{20}BAS$ were also predicted for both the transmembrane and U-shaped conformers (42), suggesting that it might be possible to detect microphase separation in these mixtures by ^{2}H NMR spectroscopy.

The potential occurrence of phase separation between bolalipids and monopolar lipids has important consequences for the appropriate design and use of bolalipids in membrane-based technologies, since lipid mixtures offer greater design flexibility in optimizing the fluidity, stability, and lateral homogeneity needed to realize functional membrane-based devices. Therefore, in this work we sought to determine whether domain formation occurs in membranes composed of $C_{20}BAS$ and POPC. Binary mixtures of $C_{20}BAS$ and POPC membranes were evaluated by solid-state ^{2}H NMR spectroscopy. We report the effects of molar ratio and temperature on $C_{20}BAS$/POPC mixed membranes using ^{2}H NMR spectroscopy, by incorporating either the deuterated bolalipid [10′, 11′-^{2}H$_2$]$C_{20}BAS$ in protiated POPC (21), or perdeuterated POPC-d$_{31}$ in protiated $C_{20}BAS$ membranes. We compared these results with data acquired by small angle x-ray scattering (SAXS) of $C_{20}BAS$/POPC membranes and computational findings from the application of molecular mean-field theory. Our evidence shows that membranes containing $C_{20}BAS$ and POPC can exhibit microphase-separated $C_{20}BAS$-rich and POPC-rich domains depending on the molar ratio of the two lipids.

MATERIALS AND METHODS

Lipid synthesis

The synthesis of $C_{20}BAS$ (37), [1′,1′,20′,20′-^{2}H$_4$]-$C_{20}BAS$, [2′,2′,19′,19′-^{2}H$_4$]$C_{20}BAS$, and [10′,11′-^{2}H$_2$]$C_{20}BAS$ (21) was previously reported.

Sample preparation for ^{2}H NMR spectroscopy

Lyophilized $C_{20}BAS$ and POPC were dissolved in 1:1 CH_3OH/$CHCl_3$ to fully mix the compounds, and the solution was then added directly to a 5-mm NMR tube. The mixture was dried under a stream of N_2 and further dried in vacuo overnight. The lipids were dispersed in ^{2}H-depleted water (^1H_2O) with 1 min of vortexing, and lyophilized. Then ^1H_2O was added to make a 50% w/w mixture. This sample was subjected to 10 freeze (liquid nitrogen), thaw (50°C), and vortex (30 s) (FTV) cycles before the ^{2}H NMR spectra were recorded. NMR tubes were closed with Teflon plugs.

^{2}H NMR spectroscopy

Solid-state ^{2}H NMR spectra were recorded using a Bruker AMX300 spectrometer (Bruker BioSpin, Karlsruhe, Germany) with a wide-bore magnet (7T) equipped with a custom-built, high-power probe (experimental details

for the spectral acquisition parameters can be found in the Supporting Material).

Data analysis for ^{2}H NMR spectroscopy

The ^{2}H NMR powder-type spectra were numerically deconvoluted, or de-Paked, to generate spectra for the $\theta = 0°$ orientation as described elsewhere (43). Details of the data analysis methods used are provided in the Supporting Material.

Samples for SAXS

Lipid mixtures (5–10 mg) were added to conical 1.5 mL polypropylene vials, sealed with o-ring screw caps, and dissolved in 1:1 CH_3OH/$CHCl_3$. The solvent was evaporated with a stream of N_2 and traces of solvent were removed in vacuo overnight. The dried lipid films were hydrated with 50% H_2O by weight and subjected to 10 FTV cycles. The samples were then fully hydrated by adding excess water (≥ 500 μL). All lipid mixtures aggregated and sank to the bottom of the conical vial. Samples were stored at $-20°C$ and allowed to equilibrate at the measurement temperature for at least 1 h before data acquisition.

SAXS measurements

SAXS measurements were performed using a fixed-anode Bruker Nanostar U system (Bruker AXS, Madison, WI) (see Supporting Material for experimental details).

Molecular theory

A molecular theory to study binary mixtures of monopolar lipids and bolalipids in the L_α phase was previously established (42). The key features of this approach are described in the Supporting Material.

RESULTS

^{2}H NMR spectroscopy of [10′,11′-^{2}H$_2$]$C_{20}BAS$/POPC mixed membranes

Three deuterated $C_{20}BAS$ derivatives—[1′,1′,20′,20′-^{2}H$_4$]$C_{20}BAS$; [2′,2′,19′,19′-^{2}H$_4$]$C_{20}BAS$; and [10′,11′-^{2}H$_2$]$C_{20}BAS$ (Fig. 1 *A*)—were synthesized as previously described (21). Multilamellar vesicle dispersions for ^{2}H NMR analysis were prepared by multiple FTV cycles before the NMR tube was loaded and spectra were acquired. Compound 1 produced two distinguishable components in the ^{2}H NMR spectrum, indicating that the two deuterium atoms at the C1′ and C20′ carbon positions were nonequivalent, consistent with previous findings for other ether-linked phospholipids (44,45). Compounds 2 and 3 gave rise to single components in the ^{2}H NMR spectra, with the corresponding order parameters of $|S_{CD}| = 0.21$ and 0.23, respectively, at 25°C (Fig. S1 in the Supporting Material).

These results demonstrate that bolalipid molecules maintain a high degree of order throughout pure bolalipid membranes. Conversely, bilayer membranes composed of monopolar lipids are significantly disordered in the center of the membrane due to the conformational freedom of the monopolar lipid acyl chains (Fig. S1) (46). These data also indicate that the bolalipids exist almost exclusively as transmembrane conformers in the membrane (i.e., configuration A_T in
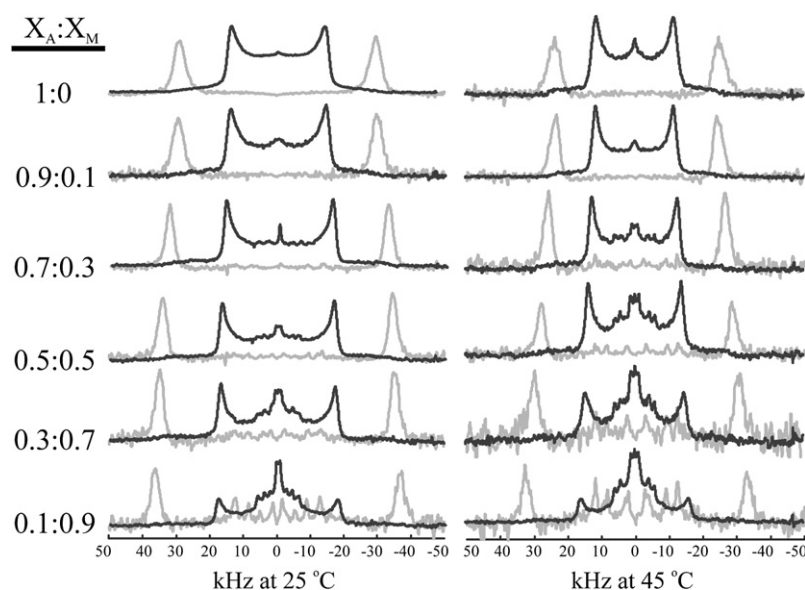
FIGURE 2 Powder-type (*black line*) and de-Paked (*gray line*) ^{2}H NMR spectra obtained from $[10',11'-^2H_2]C_{20}BAS/$ POPC (X_A/X_M) mixed membranes at various concentrations. Spectra were acquired at 25°C (*left*) and 45°C (*right*). Data for 1:0 $[10',11'-^2H_2]C_{20}BAS/POPC$ at 25°C (21) are used with permission from the American Chemical Society.

Fig. 1 *B*), where the headgroups of a single bolalipid reside on opposite leaflets of the membrane. This is inferred because the C-^{2}H bonds in the center of the transmembrane chain display higher-order parameters than the comparable position in a monopolar lipid chain, and possess an average bond orientation close to 90° relative to the membrane normal. Both of these findings are consistent with a transmembrane conformation of the *sn*-1 bolalipid chain. U-shaped conformers would give rise to significantly lower segmental order parameters in the middle of the membrane, since the orientations are less restricted than those accessible by the transmembrane conformer, providing an increased amplitude/angular range of the segmental fluctuations.

Fig. 2 shows ^{2}H NMR powder-type and de-Paked spectra for randomly oriented membranes comprised of $[10',11'-^2H_2]$ $C_{20}BAS$ and POPC binary membranes at varying molar ratios (see Table S1 in the Supporting Material for quadrupolar splittings). These data indicate that all membrane mixtures are in the L_α state at 25°C, which is expected based on the melting temperatures of $C_{20}BAS$ (17°C) and POPC (−2°C) (20,47). Membranes with X_A equal to 1, 0.9, and 0.7 (where X_A = molar ratio of $[10',11'-^2H_2]C_{20}BAS$ in the mixed membrane dispersion) give rise to ^{2}H NMR spectra with a single, large quadrupolar splitting, suggesting predominantly transmembrane bolalipids. At $X_A = 0.5$, additional components in the spectrum with small additional quadrupolar splittings become apparent. We attribute these smaller $\Delta\nu_Q$ spectral components to U-shaped $C_{20}BAS$ conformers (i.e., A_U in Fig. 1 *B*) within the membrane. As the mole fraction of $C_{20}BAS$ in the membranes decreases to 0.3 and 0.1, the contribution of the U-shaped components to the overall lineshape increases. These splittings, detectable in both the powder-type and de-Paked spectra, were more prominent at higher temperatures and were observed to be reversible. It is important to note that the component with a large quadru-

polar splitting, which we attribute to the transmembrane conformer, was the predominant species at all molar ratios.

The composition-dependent $C_{20}BAS$ order (Fig. S2) also varied as a function of temperature. As the molar ratio of $C_{20}BAS$ in the membrane increases, the quadrupolar splitting for the transmembrane component decreases. This trend is observed over a 50°C range of temperatures and at different membrane compositions (Fig. S3). As expected, the quadrupolar splittings are inversely proportional to temperature for all examined molar ratios. It should also be noted that the difference in quadrupolar splitting for different compositions decreases at sample temperatures below 10°C (i.e., as the temperature approaches the L_α–L_β phase transition of the membrane).

^{2}H NMR spectroscopy of C$_{20}$BAS/POPC-d$_{31}$ mixed membranes

Membranes composed of mixtures of perdeuterated POPC-d_{31} and fully protiated bolalipid mixtures also were evaluated at varying molar ratios (Fig. 3 *A* and Fig. S4, Table S2). At 25°C, the ^{2}H NMR spectra for all mixtures reveal an L_α membrane (Fig. 3 *A*) in which the average segmental order for methylene segments, (*i*), has the expected plateau region close to the glycerol backbone, followed by a sharp decrease in order approaching the terminal methyl group (Fig. S4). Of interest, there is no proportional relationship to the average segmental order as a function of the molar ratio of the lipids. Rather, there is an observed minimum in average segmental order for all (*i*) at $X_A = 0.3$ (Fig. 3 *B*).

At 1:1 POPC-d_{31}/C$_{20}$BAS, a coexistence of multiple POPC-d_{31} phases is detected (Fig. 4). At 10°C and above, a well-resolved L_α spectrum is observed, whereas at −60°C, a typical gel-phase spectrum is seen. Between 3°C and 7°C, however, there appear to be spectral components
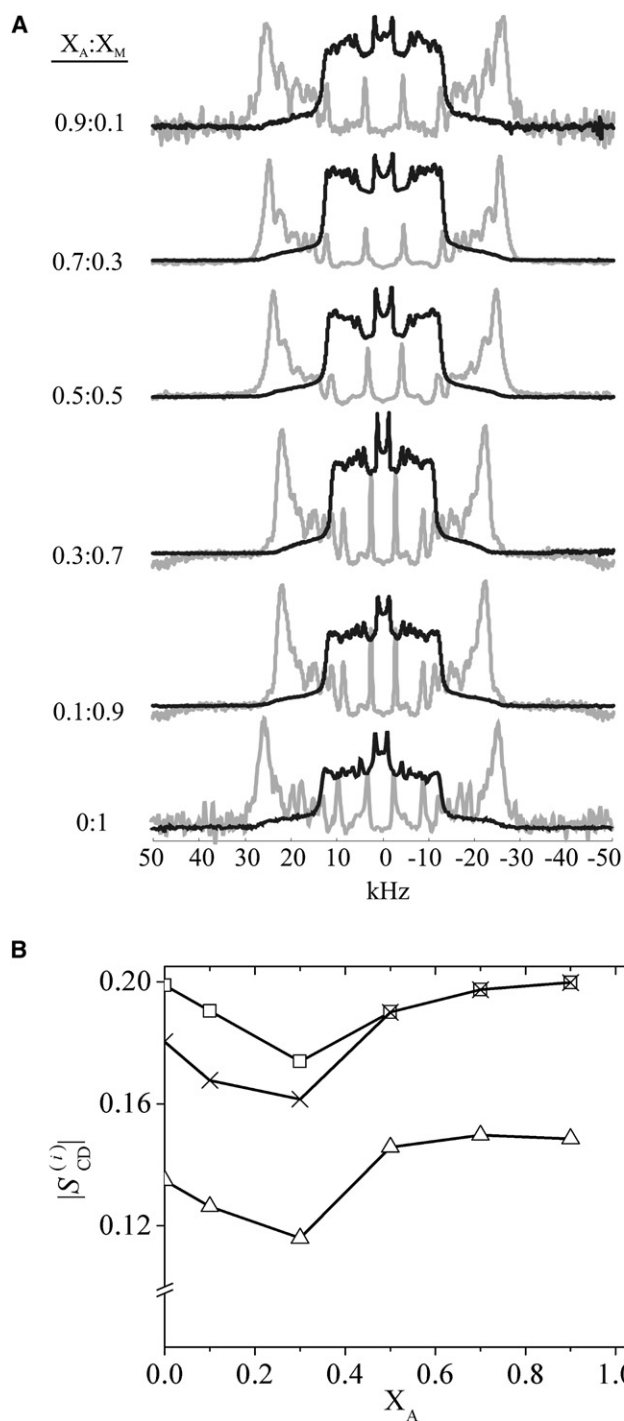
A

$X_A:X_M$

50 40 30 20 10 0 -10 -20 -30 -40 -50
kHz

B

FIGURE 3 (A) Powder-type (*black line*) and de-Paked (*gray line*) ^{2}H NMR spectra recorded for $C_{20}BAS$/POPC-d_{31} (X_A/X_M) membranes at X_A = 0.9, 0.7, 0.5, 0.3, 0.1, and 0 at 25°C. (*B*) Order parameter of [C6′] (□), [C9′] (×), and [C12′] (△) methylene units in POPC-d_{31}, as a function of $C_{20}BAS$ mole fraction in POPC at 25°C.

corresponding to POPC in the L_β and L_α phases. We attribute these observations to the formation of phase-separated domains wherein POPC-d_{31} molecules in the POPC-rich phase adopt L_α ordering, whereas POPC-d_{31} molecules that
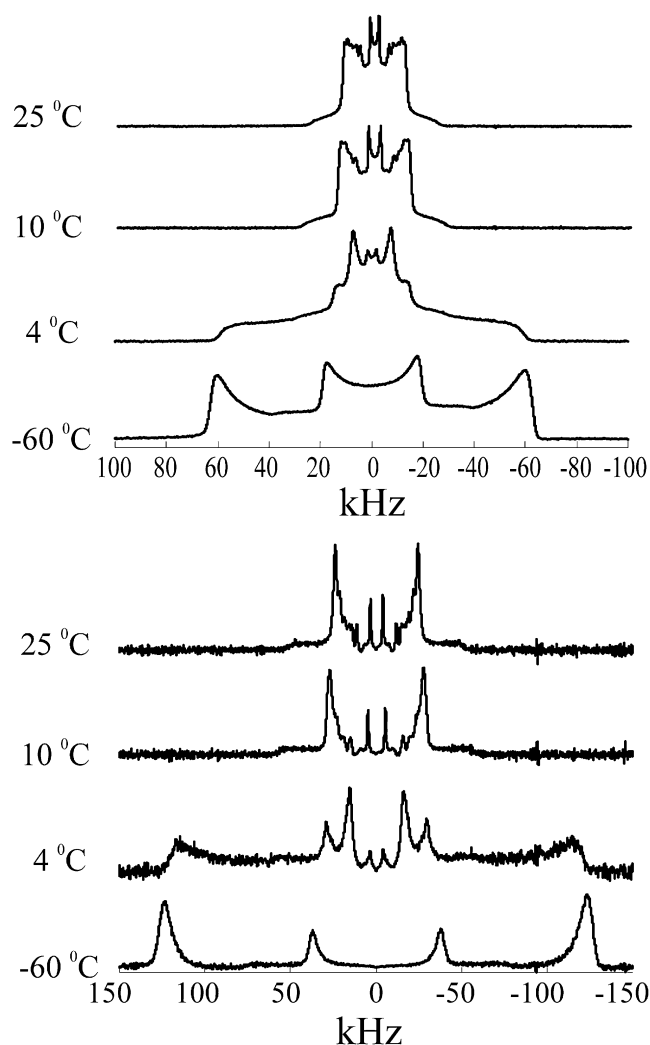

FIGURE 4 Powder (*top*) and de-Paked (*bottom*) spectra of $C_{20}BAS$/POPC-d_{31} (1:1) at 25°C, 10°C, 4°C, and −60°C.

are distributed in the bolalipid-rich phase adopt a gel phase-like ordering that is enforced by the surrounding highly-ordered bolalipids (i.e., Type III domain in Fig. 1 *D*). Under conditions of slow NMR exchange, a lower limit to the lifetime, τ, of lipids within a domain can be estimated from $\tau > 1/\Delta(\Delta\nu_Q)$, where $\Delta(\Delta\nu_Q)$ is the difference in quadrupolar splitting for the two coexisting phases. A rough lower limit to the size of a domain is then obtained using $<r^2> = 4D_L\tau$, where we introduce the mean-square distance, r, traveled in time τ for a lipid with lateral diffusion coefficient D_L. With lateral diffusion coefficients of 2×10^{-11} m^2 s^{-1} for both $C_{20}BAS$ and POPC (20,48), and $\Delta(\Delta\nu_Q) \approx 40$ kHz, we obtain a value of $<r^2>^{1/2} > 50$ nm for the lower limit to the domain size.

Molecular theory

Molecular mean-field theory (42) was used to calculate the orientational order parameters of planar mixtures of
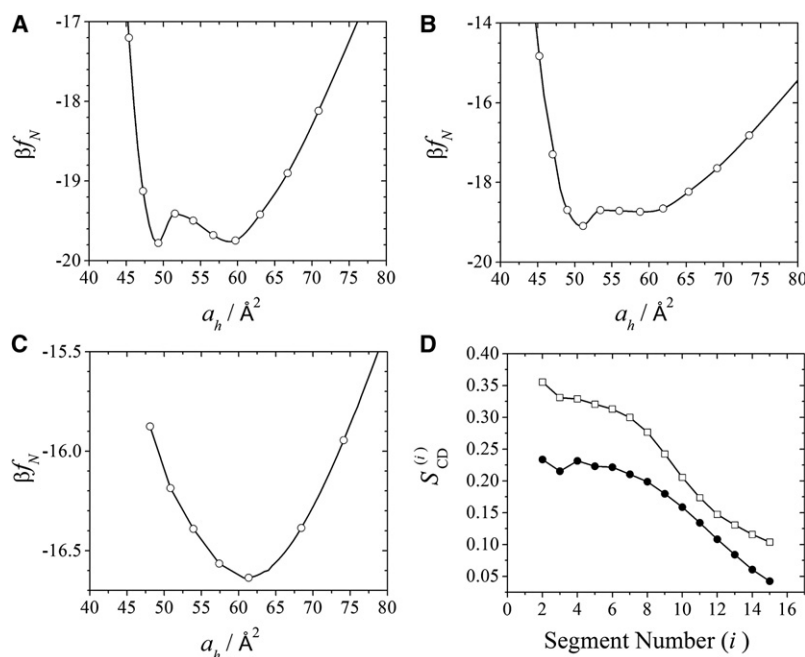
FIGURE 5 Free energy per molecule, f_N, as a function of the area per lipid headgroup, a_h, for (A) pure C_{20} BAS membranes at 17°C, the melting transition of C_{20}BAS; (B) C_{20}BAS-rich membranes ($X_A = 0.9$) in the gel phase at 4°C; and (C) POPC-rich membranes ($X_A = 0.1$) in the L_α phase at 4°C. (D) Orientational order parameters for POPC as a function of alkyl chain segment number at $X_A = 0.9$ in the gel phase (□) and $X_A = 0.1$ (•) in the L_α phase.

C_{20}BAS and POPC for comparison with the ^{2}H NMR spectral findings. In particular, we focused on the saturated sn-1-palmitoyl chain of POPC to shed more light on the lipid order parameters. The model explicitly includes conformational degrees of freedom, molecular details of the different lipid species, inhomogeneous interactions that molecules encounter within the lipid bilayer that arise from nearest-neighbor hydrophobic packing repulsions, and the alignment interactions that drive L_α–L_β phase transitions in the system. A brief description of the theoretical model used in this study is presented in the Supporting Material.

The lipid segment-segment alignment interaction strength is unknown. This parameter is adjusted in such a way that the calculated gel transition temperature of C_{20}BAS matches the experimental one of 17°C. The optimal area per lipid is not known a priori, but is determined as the area per lipid that minimizes the overall free energy. Fig. 5 A shows the free energy per molecule as a function of the area per lipid headgroup, a_h, for a pure C_{20}BAS membrane. Two local free-energy minima of equivalent magnitudes are observed, corresponding to the L_β (lower a_h) and L_α (higher a_h) phases of the pure bolalipid membrane. The fact that these two local minima are both global minima of the free energy indicates that the L_β and L_α phases coexist at this temperature.

Once this interaction parameter is set, the free energy per molecule, f_N, for mixtures of C_{20}BAS and POPC can be calculated. Fig. 5, B and C, shows f_N as a function of a_h for two mixtures with different concentrations of bolalipid: a C_{20}BAS-rich membrane ($X_A = 0.9$; Fig. 5 B) and a POPC-rich membrane ($X_A = 0.1$; Fig. 5 C). The temperature is set to 4°C to obtain more information about the mixed POPC-d$_{31}$ spectra (Fig. 4) in which both L_α- and L_β-phase

POPC components were observed. The C_{20}BAS-rich layer ($X_A = 0.9$) is clearly in the gel phase at 4°C, whereas only the higher a_h minimum is present in the POPC-rich mixture ($X_A = 0.1$), indicating that the system is in the L_α phase at this temperature. Fig. 5 D shows the orientational order parameters expected for POPC in the C_{20}BAS-rich (i.e., gel-phase; Fig. 5 B) and POPC-rich (i.e., L_α phase; Fig. 5 C) domains. Clearly, very different ^{2}H NMR spectra would be expected for POPC in these different physical environments, with the C_1-C_8 segments of the monopolar lipid acyl chain showing the greatest difference in order parameters for the L_β-like and L_α-like phase-separated domains.

SAXS patterns

SAXS patterns were acquired for membranes composed of C_{20}BAS/POPC mixtures at 30°C (Fig. 6 A). The two-dimensional x-ray patterns show uniform scattering rings, which index as the first two orders of a lamellar repeat. The scattering patterns indicate complete sample equilibration and the absence of macrophase separation for the C_{20}BAS/POPC mixtures. Radially integrated scattering profiles are shown in Fig. 6 A as a function of the scattering angle 2θ. At 30°C, the interlamellar repeat spacings reach a minimum value of 54.5 Å for $X_A = 0.9$ and a maximum value of 64.0 Å for $X_A = 0$ (Fig. 6 B). The latter value, which is for pure POPC multilayers, agrees well with previous literature (49). The temperature dependence of the D-spacing for pure C_{20}BAS membranes ($X_A = 1$) and the 1:1 mixture ($X_A = 0.5$) is shown in the Supporting Material. As the temperature increases, the D-spacing of C_{20}BAS membranes increases, whereas the D-spacing of the 1:1 mixture decreases (Fig. S5 C).
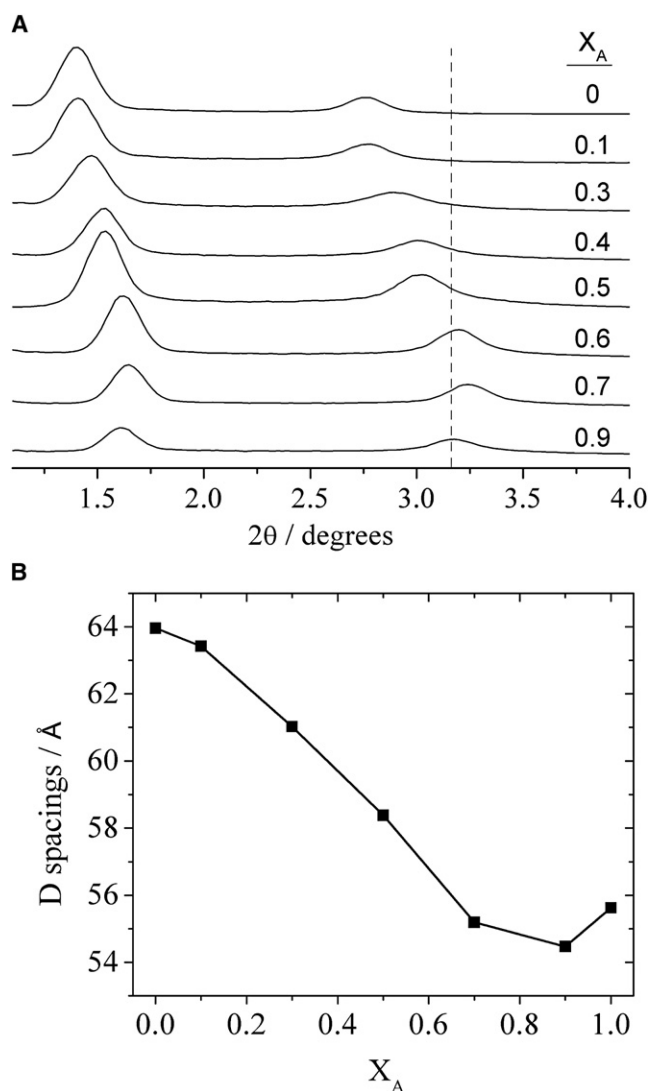
FIGURE 6 (A) SAXS patterns of $C_{20}BAS$/POPC vesicles for $X_A = 0, 0.1$, 0.3, 0.4, 0.5, 0.7, and 0.9, at 30°C. Y axis = intensity in arbitrary units. (B) D spacings of $C_{20}BAS$/POPC membranes for $X_A = 0, 0.1, 0.3, 0.5, 0.7, 0.9$, and 1.0 at 30°C.

DISCUSSION

Febo-Ayala et al. (19) previously investigated the activity of reconstituted Ste14p, an IMP enzyme with a predicted hydrophobic spanning domain of 40 Å, in $C_{20}BAS$/POPC vesicles. They found that the activity of Ste14p was not disturbed in $C_{20}BAS$/POPC mixed membranes containing low molar ratios of $C_{20}BAS$; however, above 50 mol % $C_{20}BAS$, the enzyme activity diminished dramatically. Dual-staining experiments showed that the protein was uniformly distributed in the membrane at all lipid compositions, suggesting that no macroscopic phase separation was occurring in the system. It was proposed by Febo-Ayala et al. (19) that the loss of Ste14p activity in membrane dispersions containing high molar ratios of $C_{20}BAS$ was due to a mismatch between the hydrophobic thicknesses of

the protein and the $C_{20}BAS$ membrane regimes. The nonlinearity of this relationship suggested that the bolalipid formed microphase-separated domains within POPC, such that the Ste14p activity was retained at high POPC content in the membrane by partitioning the enzyme into the thicker POPC-rich domains. In contrast, $C_{32}phytBAS$, a bolalipid that forms thicker membranes that match the hydrophobic domain of Ste14p, was capable of maintaining the activity of Ste14p at all $C_{32}phytBAS$/POPC molar ratios. Molecular theory suggests that $C_{20}BAS$ and POPC membranes, which have significantly different membrane thicknesses (32 Å (50) and 43 Å (51), respectively), undergo phase separation due to hydrophobic mismatch (42). This theory suggests that two types of domains are formed: 1), one rich in transmembrane bolalipids with a small population of POPC; and 2), one rich in POPC with a small population of U-shaped conformers (Fig. 1, B–D). ^{2}H NMR spectroscopy was used to probe for the existence of phase separation through the measurement of order parameters of bolalipids labeled with deuterium in the center of the transmembrane chain, since the order parameters of these segments should be significantly smaller if the bolalipid adopts a U-shaped conformer in the membrane instead of a transmembrane conformation.

The ^{2}H NMR spectra of $[10',11'-^{2}H_2]C_{20}BAS$/POPC membrane dispersions (Fig. 2) suggest that the bolalipid is predominantly in the transmembrane conformation for bolalipid-rich fractions (i.e., $X_A = 1, 0.9$, and 0.7). At 50 mol % $C_{20}BAS$, components in the spectra with smaller quadrupolar coupling constants begin to appear, indicating the presence of U-shaped conformers. The proportion of U-shaped bolalipids becomes more prominent as the amount of POPC in the membrane increases; however, the transmembrane component was still the predominant bolalipid conformation in the membrane even at 45°C and $X_A = 0.1$, where it accounted for ~50% of the bolalipid population. $C_{20}BAS$ is expected to be thermodynamically unstable as a transmembrane conformer in POPC-rich membranes due to significant hydrophobic mismatch; therefore, it must adopt a U-shaped conformation to become dispersed into POPC bilayers (42). Since the majority of $C_{20}BAS$ bolalipids are observed to be transmembrane conformers regardless of the $C_{20}BAS$/POPC ratio, these conformations must exist in bolalipid-rich domains that are separated from the POPC-rich domains. However, the presence of U-shaped conformers when $X_A = 0.5$ gives rise to multiple components in the ^{2}H NMR spectra with lower order parameters. This may occur because U-shaped conformers can exist in the $C_{20}BAS$-rich phase, the POPC-rich phase, and the interface between the two, potentially leading to different order parameters. Lower order parameters are expected due to the increased amplitude of segmental fluctuations near the bilayer center (46). Further, the synthesis of $[10',11'-^{2}H_2]C_{20}BAS$ produces a mixture of 16 stereoisomers (Fig. S6) that may contribute additional complexity to the ^{2}H NMR spectra. It is notable that the contributions of U-shaped conformers

were greatest at the highest temperatures studied (45°C) and that their appearance/disappearance in the sample was reversible. An additional, and somewhat surprising, observation is that the quadrupolar splitting of the transmembrane component increases with increasing mol % POPC. We attribute this finding to the effect of hydrophobic mismatch, i.e., the thicker POPC forces the bolalipid to elongate, thereby increasing the order of its alkyl chains and reducing the hydrophobic mismatch between itself and the longer POPC. This suggests that even in phase-separated domains, the POPC-rich phase promotes the extension of $C_{20}BAS$ molecules in the bolalipid-rich phase to reduce hydrophobic mismatch.

Analysis of the $C_{20}BAS$/POPC-d_{31} ^2H NMR spectra in Fig. 3 A revealed a nonlinear relationship between the order parameters for POPC-d_{31} as a function of $C_{20}BAS$ content, with a minimum observed at $X_A = 0.3$ for each methylene position analyzed (Fig. 3 B). This observation clearly shows that the membrane is heterogeneous and that very little POPC-d_{31} exists in the bolalipid-rich phase until $X_A \geq 0.5$ (i.e., where the effects of the highly ordered transmembrane bolalipid reverse the downward trend of order parameter between $X_A = 0–0.3$ and enforce more highly ordered POPC-d_{31} conformations). We attribute the decrease in POPC-d_{31} order at $X_A = 0–0.3$ to the presence of U-shaped bolalipid conformers that disrupt POPC chain packing in the POPC-rich phase. Room-temperature ^2H NMR spectra of $C_{20}BAS$/POPC-d_{31} membranes did not reveal multiple spectral components of POPC-d_{31} as a function of X_A, as was observed for $[10',11'-^2H_2]C_{20}BAS$/POPC in L_α phase bolalipid- and POPC-rich domains. Potential explanations for this finding include the possibility that the order parameter is not significantly different for POPC distributed in the two different phases (42), or that the POPC-d_{31} molecules migrate between the bolalipid- and POPC-rich domains at a rate faster than the NMR timescale.

At equimolar ratios of $C_{20}BAS$ and POPC-d_{31}, a typical gel-phase powder-type and de-Paked spectrum for POPC-d_{31} was found at −60°C (Fig. 4), which transformed into a L_α phase spectrum at temperatures of $\geq 10°C$. Evidence of coexisting L_β and L_α phases was observed, however, at intermediate temperatures, most noticeably at 4°C. We infer from this finding that POPC is populating both the bolalipid- and POPC-rich domains where the two domains exhibit different melting transitions. Since the bolalipid-rich phase is expected to have a higher T_m than the POPC-rich phase, based on the known melting transition temperatures of the corresponding pure lipid phases, POPC molecules that disperse into the bolalipid-rich phase will exist in a gel phase state at 4°C, whereas POPC present in the POPC-rich domains will exist in the L_α state at this temperature. This was the only concentration at which this phenomenon was clearly visualized, perhaps because the spectral line-broadening and weak intensities that are typical of gel-phase membranes made the signal too weak to observe at other concentrations.

We used molecular mean theory to further evaluate our ^2H NMR observations. The free energy per molecule was calculated, allowing a prediction as to whether a membrane of a given molar concentration of $C_{20}BAS$ is in the L_β or L_α phase. Using the findings of phase separation into $C_{20}BAS$-rich and POPC-rich membranes via hydrophobic mismatch as previously described (42), the expected phases for these membranes were calculated at 4°C for the $C_{20}BAS$-rich domains at $X_A = 0.9$, where gel phase lipids are predicted (Fig. 5 B), and the POPC-rich domains at $X_A = 0.1$, where a L_α phase is predicted (Fig. 5 C). Under phase-separated conditions, the ^2H NMR spectra of POPC in the L_β and L_α phases are expected to display substantially different order parameters (Fig. 5 D). Our calculations are consistent with the two-phase spectra observed in Fig. 4. It should be noted that the prediction of two different spectra for POPC is not trivial, since earlier work suggested that the spectra of POPC in the $C_{20}BAS$-rich and POPC-rich phases would not be substantially different, based on the assumption that both would be in the L_α phase (42). (The expectation of similar ^2H NMR spectra for $C_{20}BAS$-rich and POPC-rich L_α phases, analogous to the l_o and l_d phases of ternary systems, is actually observed at higher temperatures; vide supra.) Although the coexisting concentrations of the $C_{20}BAS$-rich and POPC-rich phases may be different from those predicted in Fig. 5, the structure of the lipid layers at the actual coexistence concentrations will not deviate from those calculated because the phase-separated domain structure is defined by the most abundant component (Fig. 1, B–D). Since order parameters are structural properties of the membrane lipids, the conclusions drawn from Fig. 5 about the organization of the coexisting domains remain valid.

SAXS experiments were utilized to determine the effect of bolalipid molar ratio on global phase behavior of $C_{20}BAS$/POPC mixed membranes in excess water. Two or more distinct D-spacings would be observed if macrophase-separated domains (e.g., distinct multilamellar vesicles) existed within the samples. Since a single distinct lamellar repeat distance was observed, corresponding to an ensemble average of bolalipid- and POPC-rich domains, these observations are consistent with the presence of microphase-separated domains in the mixed membrane samples, as opposed to macrophase separation. SAXS profiles were recorded for membrane mixtures at several different bolalipid contents and found to have a minimum in D-spacing at $X_A = 0.9$. The progression toward smaller repeat distances as the concentration of $C_{20}BAS$ in the membrane increases is not surprising given the smaller hydrophobic thickness of bolalipid membranes, and the expected increased stiffness based on the measured NMR order parameters. The smaller D-spacings observed at $X_A = 0.7$ and 0.9, relative to $X_A = 1$, are attributed to the effect of the low POPC molar ratios acting as an impurity in the bolalipid-rich membrane that causes thinning and lateral expansion of the membrane.

Temperature-dependent SAXS measurements were taken for membranes composed of pure $C_{20}BAS$ and 1:1 $C_{20}BAS$/POPC. Of interest, the *D*-spacings became smaller as a function of temperature for pure $C_{20}BAS$ dispersions, but increased for 1:1 $C_{20}BAS$/POPC dispersions. Two opposing mechanisms must be considered when interpreting these results: membrane thinning due to decreased order in the acyl or alkyl chains of the lipids, and increased hydration due to thermal membrane undulations, which increase the amount of water residing between membranes. We attribute the observed difference in the *D*-spacing behavior for the pure $C_{20}BAS$ and the 1:1 $C_{20}BAS$/POPC mixture to the decreased order of 1:1 $C_{20}BAS$/POPC membranes. This enables greater water penetration between the lamellar layers, and thus overwhelms the influence of increased temperature on membrane thickness. Indeed, previous temperature-dependent SAXS measurements on pure POPC membranes showed repeat distances with a minimum at 30°C (49).

CONCLUSIONS

We have demonstrated using ^{2}H NMR spectroscopy, corroborated by SAXS and molecular theory calculations, that phase separation occurs in binary mixtures of $C_{20}BAS$ and POPC. This observation is significant for guiding the design of bolalipids that will not phase-separate from monopolar lipids in membrane-based biosensors that employ lipid mixtures of this type. These findings may also be relevant for enhancing our understanding of phase-separation phenomena arising from hydrophobic mismatch in l_o/l_d domains and lipid mattressing effects in IMP/lipid mixtures.

SUPPORTING MATERIAL

Experimental methods, six figures, two tables, and references are available at http://www.biophysj.org/biophysj/supplemental/S0006-3495(09)01427-1.

REFERENCES

1. Dietrich, C., L. A. Bagatolli, Z. N. Volovyk, N. L. Thompson, M. Levi, et al. 2001. Lipid rafts reconstituted in model membranes. *Biophys. J.* 80:1417–1428.

2. Simons, K., and R. Ehehalt. 2002. Cholesterol, lipid rafts, and disease. *J. Clin. Invest.* 110:597–603.

3. Edidin, M. 2003. Timeline—lipids on the frontier: a century of cell-membrane bilayers. *Nat. Rev. Mol. Cell Biol.* 4:414–418.

4. McConnell, H., and A. Radhakrishnan. 2003. Condensed complexes of cholesterol and phospholipids. *Biochim. Biophys. Acta.* 1610:159–173.

5. London, E. 2005. How principles of domain formation in model membranes may explain ambiguities concerning lipid raft formation in cells. *Biochim. Biophys. Acta.* 1746:203–220.

6. Silvius, J. R. 2005. Partitioning of membrane molecules between raft and non-raft domains: insights from model-membrane studies. *Biochim. Biophys. Acta.* 1746:193–202.

7. Marguet, D., P. F. Lenne, H. Rigneault, and H. T. He. 2006. Dynamics in the plasma membrane: how to combine fluidity and order. *EMBO J.* 25:3446–3457.

8. Johnston, L. J. 2007. Nanoscale imaging of domains in supported lipid membranes. *Langmuir.* 23:5886–5895.

9. Veatch, S. L., I. V. Polozov, K. Gawrisch, and S. L. Keller. 2004. Liquid domains in vesicles investigated by NMR and fluorescence microscopy. *Biophys. J.* 86:2910–2922.

10. Connell, S. D., and D. A. Smith. 2006. The atomic force microscope as a tool for studying phase separation in lipid membranes. *Mol. Membr. Biol.* 23:17–28 [Review].

11. Polozov, I. V., and K. Gawrisch. 2006. Characterization of the liquid-ordered state by proton MAS NMR. *Biophys. J.* 90:2051–2061.

12. Filippov, A., G. Orädd, and G. Lindblom. 2007. Domain formation in model membranes studied by pulsed-field gradient-NMR: the role of lipid polyunsaturation. *Biophys. J.* 93:3182–3190.

13. Veatch, S. L., O. Soubias, S. L. Keller, and K. Gawrisch. 2007. Critical fluctuations in domain-forming lipid mixtures. *Proc. Natl. Acad. Sci. USA.* 104:17650–17655.

14. Bartels, T. R., S. Lankalapalli, R. Bittman, K. Beyer, and M. F. Brown. 2008. Raftlike mixtures of sphingomyelin and cholesterol investigated by solid-state ^{2}H NMR spectroscopy. *J. Am. Chem. Soc.* 130:14521–14532.

15. Simons, K., and W. L. C. Vaz. 2004. Model systems, lipid rafts, and cell membranes. *Annu. Rev. Biophys. Biomol. Struct.* 33:269–295.

16. Thompson, D. H., K. F. Wong, R. Humphry-Baker, J. J. Wheeler, J. M. Kim, et al. 1992. Tetraether bolaform amphiphiles as models of archae-bacterial membrane lipids: Raman spectroscopy, ^{31}P NMR, X-ray scattering, and electron microscopy. *J. Am. Chem. Soc.* 114:9035–9042.

17. Cornell, B. A., V. L. B. Braach-Maksvytis, L. G. King, P. D. J. Osman, B. Raguse, et al. 1997. A biosensor that uses ion-channel switches. *Nature.* 387:580–583.

18. Kim, J. M., A. Patwardhan, A. Bott, and D. H. Thompson. 2003. Preparation and electrochemical behavior of gramicidin-bipolar lipid mono-layer membranes supported on gold electrodes. *Biochim. Biophys. Acta.* 1617:10–21.

19. Febo-Ayala, W., S. L. Morera-Felix, C. A. Hrycyna, and D. H. Thompson. 2006. Functional reconstitution of the integral membrane enzyme, isoprenylcysteine carboxyl methyltransferase, in synthetic bolalipid membrane vesicles. *Biochemistry.* 45:14683–14694.

20. Febo-Ayala, W., D. P. Holland, S. A. Bradley, and D. H. Thompson. 2007. Lateral diffusion coefficients of an eicosanyl-based bisglycero-phosphocholine determined by PFG-NMR and FRAP. *Langmuir.* 23:6276–6280.

21. Holland, D. P., A. V. Struts, M. F. Brown, and D. H. Thompson. 2008. Bolalipid membrane structure revealed by solid-state ^{2}H NMR spectroscopy. *J. Am. Chem. Soc.* 130:4584–4585.

22. De Rosa, M., and A. Gambacorta. 1988. The lipids of archaebacteria. *Prog. Lipid Res.* 27:153–175.

23. Benvegnu, T., M. Brard, and D. Plusquellec. 2004. Archaeabacteria bipolar lipid analogues: structure, synthesis and lyotropic properties. *Curr. Opin. Colloid Interface Sci.* 8:469–479.

24. Damste, J. S. S., S. Schouten, E. C. Hopmans, A. C. T. van Duin, and J. A. J. Geenevasen. 2002. Crenarchaeol: the characteristic core glycerol dibiphytanyl glycerol tetraether membrane lipid of cosmopolitan pelagic crenarchaeota. *J. Lipid Res.* 43:1641–1651.

25. Fuhrhop, A. H., and T. Y. Wang. 2004. Bolaamphiphiles. *Chem. Rev.* 104:2901–2937.

26. Sun, X. L., N. Biswas, T. Kai, Z. F. Dai, R. A. Dluhy, et al. 2006. Membrane-mimetic films of asymmetric phosphatidylcholine lipid bolaamphiphiles. *Langmuir.* 22:1201–1208.

27. Patel, G. B., and G. D. Sprott. 1999. Archaeobacterial ether lipid liposomes (archaeosomes) as novel vaccine and drug delivery systems. *Crit. Rev. Biotechnol.* 19:317–357.

28. Denoyelle, S., A. Polidori, M. Brunelle, P. Y. Vuillaume, S. Laurent, et al. 2006. Synthesis and preliminary biological studies of hemifluori-nated bifunctional bolaamphiphiles designed for gene delivery. *New J. Chem.* 30:629–646.

29. Rethore, G., T. Montier, T. Le Gall, P. Delepine, S. Cammas-Marion, et al. 2007. Archaeosomes based on synthetic tetraether-like lipids as novel versatile gene delivery systems. *Chem. Commun. (Camb.).* 20:2054–2056.

30. Benvegnu, T., and L. L. S. Cammas-Marion. 2008. Archaeal lipids: innovative materials for biotechnological applications. *Eur. J. Org. Chem.* 2008:4725–4744.

31. Elferink, M. G. L., J. G. Dewit, R. Demel, A. J. M. Driessen, and W. N. Konings. 1992. Functional reconstitution of membrane-proteins in monolayer liposomes from bipolar lipids of sulfolobus-acidocaldarius. *J. Biol. Chem.* 267:1375–1381.

32. Veld, G. I., M. G. L. Elferink, A. J. M. Driessen, and W. N. Konings. 1992. Reconstitution of the leucine transport-system of lactococcus-lac-tis into liposomes composed of membrane-spanning lipids from sulfolo-bus-acidocaldarius. *Biochemistry.* 31:12493–12499.

33. Huguet, C., E. C. Hopmans, W. Febo-Ayala, D. H. Thompson, J. S. S. Damste, et al. 2006. An improved method to determine the absolute abundance of glycerol dibiphytanyl glycerol tetraether lipids. *Org. Geo-chem.* 37:1036–1041.

34. Grather, O., and D. Arigoni. 1995. Detection of regioisomeric macrocy-clic tetraethers in the lipids of methanobacterium-thermoautotrophicum and other archaeal organisms. *J. Chem. Soc. Chem. Commun.* 4:405–406.

35. Svenson, S., and D. H. Thompson. 1998. Facile and efficient synthesis of bolaamphiphilic tetraether phosphocholines. *J. Org. Chem.* 63:7180–7182.

36. Wang, G. J., and R. I. Hollingsworth. 1999. Synthesis and properties of a bipolar, bisphosphatidyl ethanolamine that forms stable 2-dimensional self-assembled bilayer systems and liposomes. *J. Org. Chem.* 64:4140–4147.

37. Patwardhan, A. P., and D. H. Thompson. 2000. Novel flexible and rigid tetraether acyclic and macrocyclic bisphosphocholines: synthesis and monolayer properties. *Langmuir.* 16:10340–10350.

38. Kai, T., X. L. Sun, K. M. Faucher, R. P. Apkarian, and E. L. Chaikof. 2005. Design and synthesis of asymmetric acyclic phospholipid bolaamphiphiles. *J. Org. Chem.* 70:2606–2615.

39. Melikyan, G. B., N. S. Matinyan, S. L. Kocharov, V. B. Arakelian, D. A. Prangishvili, et al. 1991. Electromechanical stability of planar lipid-membranes from bipolar lipids of the thermoacidophilic archebacte-rium sulfolobus-acidocaldarius. *Biochim. Biophys. Acta.* 1068:245–248.

40. Delfino, J. M., S. L. Schreiber, and F. M. Richards. 1993. Design, synthesis, and properties of a photoactivatable membrane-spanning phospholipidic probe. *J. Am. Chem. Soc.* 115:3458–3474.

41. Cuccia, L. A., F. Morin, A. Beck, N. Hebert, G. Just, et al. 2000. Span-ning or looping? The order and conformation of bipolar phospholipids in lipid membranes using ^{2}H NMR spectroscopy. *Chem. Eur. J.* 6:4379–4384.

42. Longo, G. S., D. H. Thompson, and I. Szleifer. 2007. Stability and phase separation in mixed monopolar lipid/bolalipid layers. *Biophys. J.* 93:2609–2621.

43. McCabe, M. A., and S. R. Wassall. 1995. Fast-Fourier-transform depak-ing. *J. Magn. Reson. B.* 106:80–82.

44. Ruocco, M. J., A. Makriyannis, D. J. Siminovitch, and R. G. Griffin. 1985. Deuterium NMR investigation of ether-linked and ester-linked phosphatidylcholine bilayers. *Biochemistry (Mosc.).* 24:4844–4851.

45. Stewart, L. C., M. Kates, I. H. Ekiel, and I. C. P. Smith. 1990. Molecular order and dynamics of diphytanylglycerol phospholipids—a ^{2}H-NMR and ^{31}P-NMR study. *Chem. Phys. Lipids.* 54:115–129.

46. Petrache, H. I., S. W. Dodd, and M. F. Brown. 2000. Area per lipid and acyl length distributions in fluid phosphatidylcholines determined by ^{2}H NMR spectroscopy. *Biophys. J.* 79:3172–3192.

47. Silvius, J. R. 1982. Thermotropic phase transitions of pure lipids in model membranes and their modifications by membrane proteins. *In* Lipid-Protein Interactions. P. C. Jost and O. H. Griffith, editors. John Wiley and Sons, New York.

48. Lindblom, G., L. B. Å. Johansson, and G. Arvidson. 1981. Effect of cholesterol in membranes. Pulsed nuclear magnetic resonance measure-ments of lipid lateral diffusion. *Biochemistry.* 20:2204–2207.

49. Pabst, G., M. Rappolt, H. Amenitsch, S. Bernstorff, and P. Laggner. 2000. X-ray kinematography of temperature-jump relaxation probes the elastic properties of fluid bilayers. *Langmuir.* 2000:8994–9001.

50. Meglio, C. D., S. B. Rananacare, S. Svenson, and D. H. Thompson. 2000. Bolaamphiphilic phosphocholines: structure and phase behavior in aqueous media. *Langmuir.* 16:128–133.

51. Caffrey, M., and G. W. Fiegenson. 1981. Fluorescence quenching in model membranes. 3. Relationship between calcium adenosine-triphos-phatase enzyme-activity and the affinity of the protein for phosphatidy-cholines with different acyl chain characteristics. *Biochemistry.* 20:1949–1961.